

Electrochemical characterization of binary carbon supported electrode in polymer electrolyte fuel cells

Xin Wang, I-Ming Hsing*, P.L. Yue

Department of Chemical Engineering, Hong Kong University of Science and Technology, Clear Water Bay, Kowloon, Hong Kong, PR China

Received 4 April 2000; received in revised form 9 June 2000; accepted 9 October 2000

Abstract

In this paper, we report the use of binary carbon supports for fabricating electrodes of polymer electrolyte fuel cells and their detailed electrochemical characterization. The introduction of a secondary support in electrode is shown to provide a combination of high conductivity and good surface morphology. Cyclic voltammetry and cell polarization test indicate that the electrode prepared by binary carbon supports offers more catalytic sites and thus gives a better performance than that of single support. Comparison of kinetic parameters obtained from the model fitting shows that the improvement is not only due to the increased Pt active surface area, but also attributed to the enhanced kinetics, which is further supported by the decreased activation energy for ORR on binary-support electrode. Through the determination of pressure effect, reaction order of ORR with respect to O₂ is identified to be unity, which is in agreement with other researcher's result. © 2001 Elsevier Science B.V. All rights reserved.

Keywords: Polymer electrolyte fuel cells; Binary carbon supports; Gas diffusion electrode; Electrode kinetics

1. Introduction

More and more attention has been paid to polymer electrolyte fuel cells (PEFCs) as a power source for residential and transportation applications because of their high energy-conversion efficiency and near-zero pollutant emission [1]. Over the past years, research has been devoted to lowering catalyst loading and electrode overpotential losses. A significant progress on electrode development was first made by Raistrick [2]. They impregnated the gas diffusion electrode originally for phosphoric acid fuel cells with electrolyte ionomer, which resulted in a 10-fold reduction of catalyst loading. Ticianelli and coworkers [3,4] made a further improvement to localize Pt catalyst near the front surface of electrode by employing a high wt.% Pt supported on carbon and sputtering a thin layer of Pt on electrode surface. Later, noticeable advances were made by Wilson and coworkers [5,6], who mixed solubilized electrolyte ionomer with Pt/C to form catalyst layer, and applied it to the electrode or membrane. They reported a contact area increase and performance improvement by this mode of fabrication.

In addition to issues related to the electrocatalyst, structure and property of carbon support is also important because it contributes to the overall performance of the electrode. Carbon is not only used to conduct electrons and serves as a catalyst carrier, but also helps to the stabilization of three-phase boundary and morphology [7]. The use of various graphite and carbon black materials as a single catalyst support for electrodes has been reported. However, with a single carbon support it may not be easy to tailor electrode structure to achieve a combination of high conductivity, good morphology, and suitable hydrophobicity. Sakaguchi et al. [8] and Watanabe and Makita [9] first approached the idea of adopting binary carbon supports for the use in liquid electrolyte fuel cells. They have demonstrated an improved utilization of Pt catalyst using this approach.

In this paper, we extend their efforts by employing binary carbon supports to fabricate thin film electrode in PEFCs. The role of binary carbon supports inside the membrane and electrode assembly (MEA) will be evaluated and characterized through measurements of cell polarization and in situ cyclic voltammetry (CV). It will be shown that with the use of two carbon supports, cell performance and active surface area of the electrode can be enhanced. This improvement is further exemplified by the enhanced electrode kinetics of oxygen reduction reaction (ORR) for binary-support electrode compared to that with single support.

* Corresponding author. Tel.: +852-2358-7131; fax: +852-2358-0054.
E-mail address: kehsing@ust.hk (I.-M. Hsing).

2. Experimental

2.1. Membrane and electrode assembly preparation

Membrane and electrode assemblies (MEAs) were prepared according to the procedures described by Wilson [5,6] except that, instead of using single carbon support (Vulcan XC-72, surface area $254 \text{ m}^2/\text{g}$ and particle size 30 nm), two carbon supports (Vulcan XC-72 (VC) and black Pearl 2000 (BP) with surface area $1475 \text{ m}^2/\text{g}$ and particle size 15 nm) were used in our study. Briefly, 20 wt.% Pt supported on Vulcan XC-72 (VC) and on Black pearl 2000 (BP) were mixed at the ratio of nine to one, which gives a specific surface area of 376 cm^2 . It was then ultrasonically mixed with 5 wt.% Nafion solution (DuPont) and de-ionized water at the mass ratio of 3:1:5 to form viscous ink, which was subsequently brushed on to an uncatalyzed E-TEK electrode. Measuring the weight difference of electrode before and after brushing, Pt loading of this electrode was determined to be 0.20 mg/cm^2 . Used as cathode, the catalyzed electrode was hot-pressed to Nafion 117 membrane and 0.35 mg/cm^2 E-TEK anode at 135°C and 80 atm for one and half minutes to form MEA. Before the hot pressing, Nafion membrane was pretreated with a reported procedure to remove organic impurities and metal ion contaminants [3] and a thin Nafion layer was brushed on to the interfaces between electrodes and membrane.

2.2. Cell polarization measurement

An FCT-2000 fuel cell test station (ElectroChem, USA) was used to measure cell polarization of a 5 cm^2 single fuel cell with the serpentine flow pattern. H_2 and oxidant (O_2 or air) streams were humidified by passing through a temperature controlled humidifier before feeding to the fuel cell. Humidification temperatures of feed streams at the anode and cathode are 15 and 10°C , respectively, higher than the cell temperature. Unless otherwise specified, reactant gas flow rates were adjusted to a constant 5 stoichiometry with a minimum flow rate of 70 and 40 ml/min for hydrogen and oxygen, respectively. Total gas pressure was regulated by back-pressure regulators. Applied loading, fuel mass flow rates, and cell temperatures were digitally controlled.

2.3. Cyclic voltammetry

In situ cyclic voltammetry was conducted using a computer controlled Autolab potentiostat (Eco Chemie, The Netherlands) with Ar passing through the cathode (working electrode) and H_2 passing through the anode (counter electrode) at 50°C and 1 atm. The potential was cycled at 100 mV/s between 0 and $+1.0 \text{ V}$ (versus RHE) until a stable voltammogram was obtained. Humidifier temperature for the experiments was set at 70°C and the flow rates of both gases were fixed at 40 ml/min. Counter electrode is also served as a reference electrode because of its negligible

overpotential [10–13]. Active surface area of Pt can be obtained by measuring the charge required for hydrogen desorption from the Pt surface after subtracting double layer capacitance from the voltammogram and employing monolayer adsorption charge of $210 \mu\text{C}/\text{cm}^2$ for a smooth Pt electrode. Two parameters were calculated in CV measurements. One is the roughness factor defined as the ratio of the electrochemically active surface area to the geometric surface area. The other is the utilization efficiency of Pt, which is termed as the ratio between the measured surface area and the calculated total Pt surface area. The total Pt surface area is calculated based on an average particle size of 3.5 nm and a cubo-octahedron cluster model which gives a corresponding total surface area of $88.7 \text{ m}^2/\text{g}$ [14].

3. Result and discussion

3.1. CV measurement and cell polarization testing

Cyclic voltammetric measurements for binary- and single-support electrodes are shown in Fig. 1. The improved active surface area can be observed by the comparison of calculated values of roughness factors which are 70 and 95 for electrodes with single- and binary-support, respectively. And the Pt utilization efficiency is increased from 40 to 54% with the use of binary-support. As a result, binary-support electrode exhibits a better performance than that with single carbon support as shown in Fig. 2. It is believed that the improvement in the binary electrode is resulted from a better contact between Pt and electrolyte ionomer provided by the blending of BP carbon. BP materials have different structural properties from VC. As they are mixed together with electrolyte Nafion ionomer, smaller BP particles are expected to occupy the voids inside or between agglomerates formed

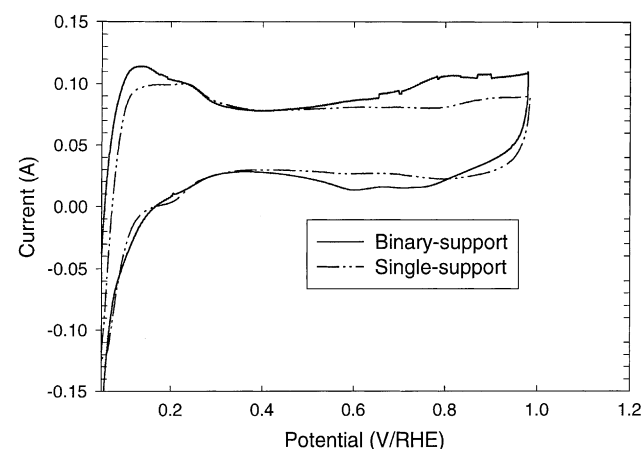


Fig. 1. In situ cyclic voltammogram for single- and binary-support electrode. Pt loading in cathode and anode are 0.2 and 0.35 mg/cm^2 , respectively. Operating conditions: cell temperature, 50°C ; humidifier temperature, 70°C ; atmospheric pressure; H_2 flow rate 40 sccm/min ; Ar flow rate 40 sccm/min and scan rate 100 mV/s .

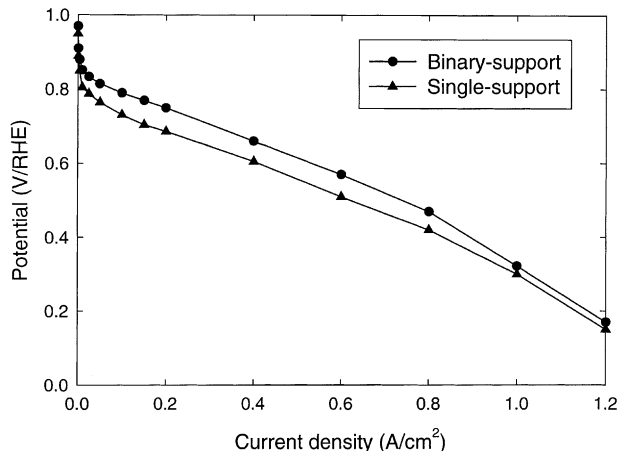


Fig. 2. Cell polarization curves for single- and binary-support electrode. Pt loading in cathode and anode are 0.2 and 0.35 mg/cm^2 , respectively. Operating conditions: cell temperature, 60°C ; atmospheric pressure; O_2 and H_2 flow rate at 5 stoichiometry.

by larger VC particles. Consequently, the highly conductive BP particles bridge the separated conductive paths, and thus the electronic conductivity of the electrode is increased. From the viewpoint of tailoring surface properties, BP powder in possession of high surface area and capability to adsorb water offers a better contact with electrolyte ionomer than does VC, helping VC carbon retain sufficient water to enhance the ionic conductivity of the electrode. The combination of increased electronic and ionic conductivity contributes to the better cell polarization characteristics of MEA with binary-support electrode.

3.2. Tafel parameters for single- and binary-support electrodes

Based on the cell polarization data shown in Fig. 2, kinetic parameters of ORR for MEAs with single- and binary-support electrodes can be obtained from an empirical Tafel equation [3]:

$$E = E_0 - b \log(i) - Ri \quad (1)$$

where

$$E_0 = E_r + b \log(i_0), \quad (2)$$

b and i_0 are Tafel slope and exchange current density for the ORR, respectively, R the slope of the linear region of E versus i plot, which represents the resistance including the predominant membrane ohmic resistance, contact resistance and charge transfer resistance of the hydrogen electrode, and E_r the reversible potential of ORR corrected for temperature and pressure influence [15].

Electrode kinetic parameters estimated by the least squares fitting procedure are summarized in Table 1. Binary-support electrode, as expected, shows a lower Tafel slope b and a higher exchange current density based on geometric area (i_0), reconfirming its better performance than that of single-support electrode. The exchange current density based on actual active surface of the electrode i_0^* was obtained by dividing i_0 with roughness factor. This value is also higher for binary-support electrode (1.30×10^{-7} versus $2.32 \times 10^{-7} \text{ mA/cm}^2$), which means the improvement in performance is not only due to the increase in active surface area of Pt, but also due to the contribution of improvement from kinetics. Values of resistance R for both electrodes obtained from the nonlinear fitting agree closely with the measurement of membrane ohmic resistance R_{hf} at high frequency of 10 kHz (0.290 and $0.276 \Omega \text{ cm}^2$ for single- and binary-support electrode, respectively).

3.3. Effect of temperature on electrode kinetic parameters

Polarization data for binary- and single-support electrodes at different cell temperatures were nonlinearly fitted in the same way as described in the previous section and their results are also listed in Table 1. iR -corrected Tafel plots (Figs. 3 and 4) for both electrodes show that Tafel slope is weakly dependent on the temperatures as previously reported [16]. The difference between Figs. 3 and 4 is that the change of E_0 with respect to temperature is bigger for the single-support electrode than for the binary-support electrode. This difference can also be observed from the values of exchange current densities as listed in Table 1. The

Table 1

Electrode kinetic parameters for ORR on binary- and single-support electrodes under different temperatures^a

Temperature ($^\circ\text{C}$)	E_r (mV)	E_0 (mV)	b (mV/dec)	R ($\Omega \text{ cm}^2$)	i_0 (mA/cm^2)
Binary-support					
40	1213	905	58.6	0.282	3.53×10^{-6}
50	1204	915	57.9	0.275	1.01×10^{-5}
60	1195	923	58.4	0.268	2.20×10^{-5}
70	1186	928	59.8	0.262	4.78×10^{-5}
Single-support					
40	1213	865	61	0.298	1.31×10^{-6}
50	1204	874	59.4	0.292	3.96×10^{-6}
60	1195	889	60.7	0.285	9.09×10^{-6}
70	1186	912	62	0.280	2.58×10^{-5}

^a Operating condition: atmospheric pressure.

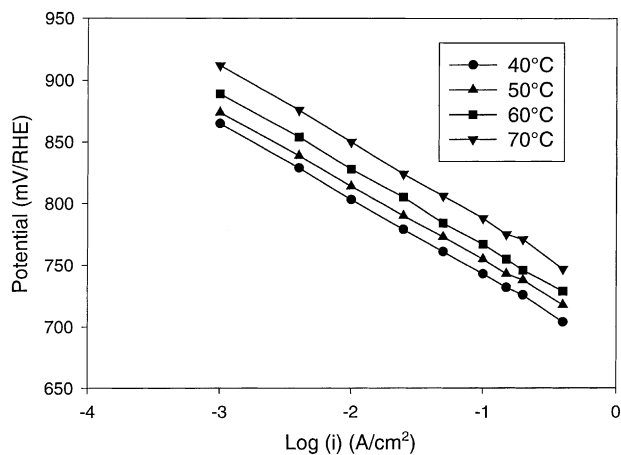


Fig. 3. iR -corrected Tafel plots at different temperature for single-support electrode. Pt loading in cathode and anode are 0.2 and 0.35 mg/cm², respectively. Operating conditions: atmospheric pressure; O_2 and H_2 flow rate at 5 stoichiometry.

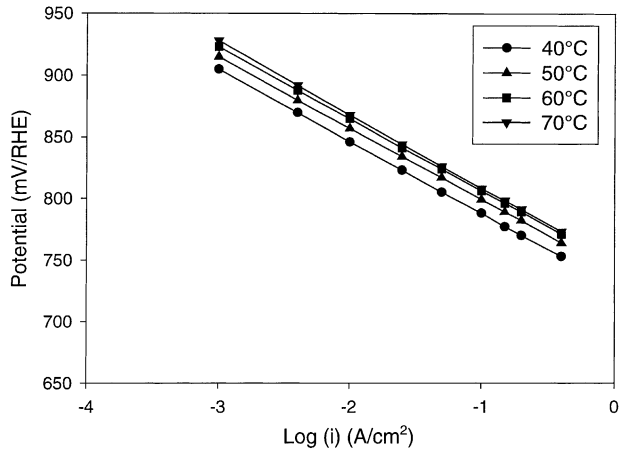


Fig. 4. iR -corrected Tafel plots at different temperature for binary-support electrode. Pt loading in cathode and anode are 0.2 and 0.35 mg/cm², respectively. Operating conditions: atmospheric pressure; O_2 and H_2 flow rate at 5 stoichiometry.

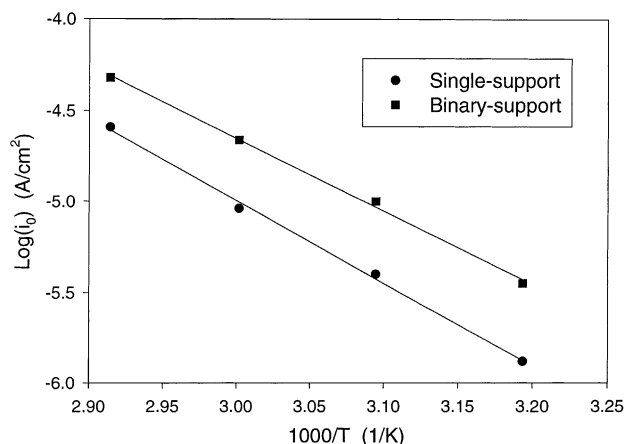


Fig. 5. Plot of $\log i_0$ vs. $1/T$ for ORR on both single- and binary-support electrodes (Arrhenius plot). Pt loadings in cathode and anode are 0.2 and 0.35 mg/cm², respectively. Operating conditions: atmospheric pressure; O_2 and H_2 flow rate at 5 stoichiometry.

temperature dependence of the exchange current density can be evaluated by a typical Arrhenius plotting as shown in Fig. 5. The activation energies E_a of 77 and 87 kJ/mol for binary- and single-support electrode, respectively, are yielded from the slope of the plot via

$$E_a = -2.303R \frac{d(\log i_0)}{d(1/T)} \quad (3)$$

Binary-support electrode offers an enhanced kinetics of ORR as exemplified by the lower activation energy, thus improving the cell polarization characteristics of MEA.

3.4. Effect of pressure on electrode kinetic parameters

Effect of pressure on electrode kinetic parameters were evaluated in a similar manner as was done for the determination of temperature effects and its results are delineated in Table 2. Similar to the temperature effect, the Tafel slopes

Table 2

Electrode kinetic parameters for ORR on binary- and single-support electrodes under different pressures^a

Pressure (atm)	E_r (mV)	E_0 (mV)	b (mV/dec)	R ($\Omega \text{ cm}^2$)	i_0 (mA/cm^2)
Binary-support					
1	1186	928	59.8	0.262	4.78×10^{-5}
2	1192	948	60.3	0.259	1.05×10^{-4}
3	1196	964	58.7	0.257	1.66×10^{-4}
4	1198	970	59.4	0.256	2.40×10^{-4}
5	1200	979	59.6	0.256	2.82×10^{-4}
Single-support					
1	1186	912	62	0.280	2.58×10^{-5}
2	1192	934	61.5	0.277	5.62×10^{-5}
3	1196	949	60.4	0.275	9.33×10^{-5}
4	1198	954	61.3	0.275	1.20×10^{-4}
5	1200	964	60.8	0.274	1.55×10^{-4}

^a Operating condition: 70°C.

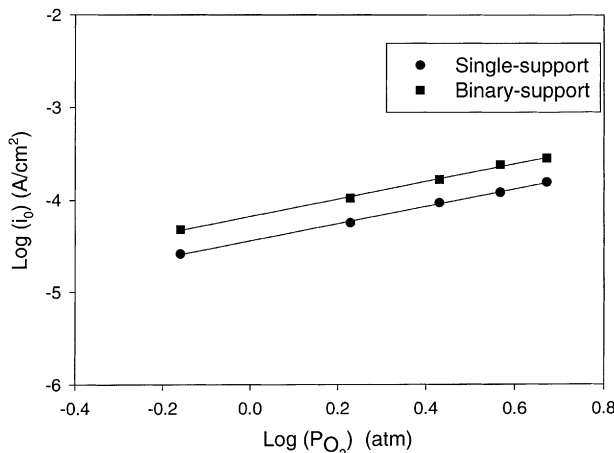


Fig. 6. Comparison of pressure effect on exchange current density i_0 for binary- and single-support electrode. Pt loadings in cathode and anode are 0.2 and 0.35 mg/cm², respectively. Operating conditions: 70°C; O₂ and H₂ flow rate at 5 stoichiometry.

are almost unchanged for both electrodes under various pressure conditions. To identify pressure effects to oxygen kinetics for both electrodes, relations of $\log i_0$ and E_0 versus $\log(P_{O_2})$ are plotted in Figs. 6 and 7. Slopes of $\log i_0$ versus $\log(P_{O_2})$ for both electrodes are close to unity, indicating that the rate of ORR with respect to O₂ concentration is the first-order. Same conclusion can be obtained from the analysis of plots of E_0 versus $\log(P_{O_2})$, which gives two almost parallel lines for both electrodes with slope of about 60 mV/dec. Because for a n th-order reaction, the following equation is valid:

$$\left(\frac{\partial E}{\partial \log(P_{O_2})} \right)_i = b \times n_{O_2} \quad (4)$$

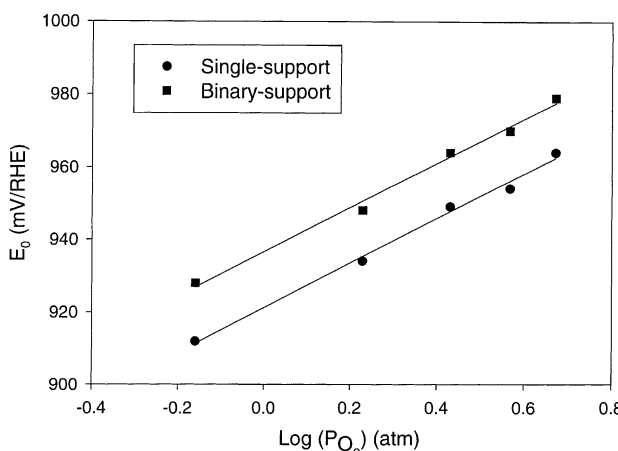
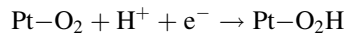


Fig. 7. Comparison of pressure effect on E_0 for binary- and single-support electrode. Pt loadings in cathode and anode are 0.2 and 0.35 mg/cm², respectively. Operating conditions: 70°C; O₂ and H₂ flow rate at 5 stoichiometry.

where n_{O_2} is the reaction order of O₂, it is obvious that the slope of the lines in Fig. 7 equals to the product of the Tafel slope and the reaction order for ORR. As we already know from the experiments that the Tafel slope is about 60 mV/dec, so the reaction order necessarily has to be unity. Same results have been reported on Nafion impregnated E-TEK electrode and Pt microelectrode [17,18], which means the reaction order of ORR with respect to O₂ is inherently unity no matter what kind of form the catalyst is. They also proposed a rate-determining step for the ORR in Pt surface.



In consideration of similar Tafel slope, activation energy and reaction order obtained in this work compared with theirs [17,18], it is reasonable to assume that this mechanism will also be valid for the binary-support electrode.

4. Conclusions

It is concluded that binary-support electrode demonstrates an improved polarization performance than single-support electrode. The CV results show that binary-support electrode provides more active catalytic sites than the single-support electrode under the same Pt loading conditions and thus enhance Pt utilization efficiency by 14%. Comparison of kinetics parameters for both electrodes indicates that the improvement is not only due to the increase of active surface area but also attributed to the enhanced ORR kinetics. This observation is also supported by the decreased activation energy for ORR with binary-support electrode from the analysis of temperature dependence on electrode kinetic parameters. The pressure dependence shows that the reaction order for ORR with respect to oxygen is determined to be unity, which is in agreement with other researchers' results [17,18].

Acknowledgements

The authors gratefully acknowledge Hong Kong Research Grants Council (HKUST6042/00P) for the initial funding support. Technical assistance from Mr. K.H. Kwok is also appreciated.

References

- [1] S. Srinivasan, J. Electrochem. Soc. 136 (1989) 41C.
- [2] I.D. Raistrick, in: J.W. Zee, R.E. White, K. Kinoshita, H.S. Burney (Eds.), *Proceedings of the Symposium on Diaphragms, Separators, and Ion Exchange Membranes*, The electrochemical Society, Princeton, NJ, 1986, p. 172.
- [3] E.A. Ticianelli, C.R. Derouin, S. Srinivasan, J. Electroanal. Chem. 251 (1988) 275.
- [4] S. Mukerjee, S. Srinivasan, *Electrochim. Acta* 38 (1988) 1661.
- [5] M.S. Wilson, US Patent 5,211,984 (1993).
- [6] M.S. Wilson, *Electrochim. Acta* 40 (1995) 355.

- [7] X. Xu, Polymer/carbon blend electrodes and polyphosphonate membrane for PEM fuel cells, Thesis, State University of New York, NY, 1993.
- [8] M. Sakaguchi, K. Uematsu, A. Sakata, *Electrochim. Acta* 34 (1989) 625.
- [9] M. Watanabe, K. Makita, *J. Electroanal. Chem.* 197 (1986) 195.
- [10] S. Escribano, P. Aldebert, *Solid State Ionics* 77 (1995) 318.
- [11] R.L. Borup, N.E. Vandeborgh, Characterization of PEM fuel cell MEA by electrochemical methods and microanalysis, *Electrochem. Soc. Proc.* (1995).
- [12] T.R. Ralph, G.A. Hards, *J. Electrochem. Soc.* 144 (1997) 3845.
- [13] O.J. Murphy, *J. Power Sources* 47 (1994) 353.
- [14] S.J. Lee, S. Mukerjee, *Electrochim. Acta* 43 (1998) 3693.
- [15] A. Parthasarathy, C.R. Martin, S. Srinivasan, *J. Electrochem. Soc.* 138 (1997) 916.
- [16] M.A. Enayetullah, T.D. Devilbiss, *J. Electrochem. Soc.* 136 (1989) 3369.
- [17] A. Pathasarathy, S. Srinivasan, *J. Electrochem. Soc.* 139 (1992) 2856.
- [18] S. Srinivasan, *J. Electroanal. Chem.* 357 (1993) 201.